

Supplementary Materials for  
**Reconstructing codependent cellular cross-talk in lung adenocarcinoma  
using REMI**

Alice Yu, Yuanyuan Li, Irene Li, Michael G. Ozawa, Christine Yeh, Aaron E. Chiou,  
Winston L. Trope, Jonathan Taylor, Joseph Shrager, Sylvia K. Plevritis\*

\*Corresponding author. Email: [sylvia.plevritis@stanford.edu](mailto:sylvia.plevritis@stanford.edu)

Published 18 March 2022, *Sci. Adv.* **8**, eabi4757 (2022)  
DOI: [10.1126/sciadv.abi4757](https://doi.org/10.1126/sciadv.abi4757)

**The PDF file includes:**

Figs. S1 to S6  
Legends for data files S1 to S6

**Other Supplementary Material for this manuscript includes the following:**

Data files S1 to S6

## Supplementary Figures

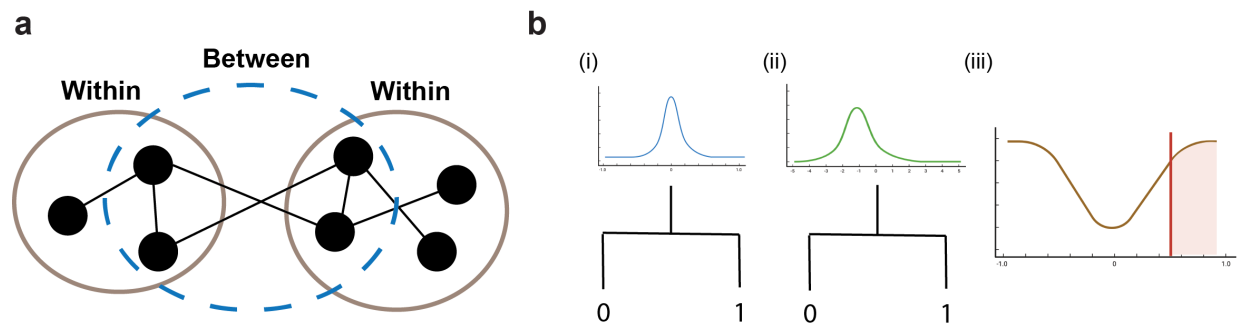


**Fig. S1. Diagram of REMI intermediate steps. (a)** Schematic of an overlapping community that captures edges between communities. **(b)** Diagram of steps to calculate p-value for a given ligand-receptor edge. (i) Sampling correlation values to replace edge of interest and creating a tree to predict whether edge appears or not in REMI network. (ii) Sampling from null inverse Wilshart distribution and using classification trees to predict whether edge is present or not (iii) Calculating number of randomly sampled edge values with higher predicted correlation than correlation from true data to estimate two-sided p-value.

**a**

| Cohort Size<br>( $n$ ) | Within      |             | Between     |             |
|------------------------|-------------|-------------|-------------|-------------|
|                        | Sensitivity | Specificity | Sensitivity | Specificity |
| 15                     | 0.75        | 0.45        | 0.45        | 0.76        |
| 25                     | 0.78        | 0.48        | 0.49        | 0.78        |
| 50                     | 0.84        | 0.50        | 0.62        | 0.75        |
| 100                    | 0.89        | 0.55        | 0.76        | 0.73        |
| 200                    | 0.93        | 0.63        | 0.88        | 0.74        |

**b**

| Community Size<br>( $n$ = Sample Size) | REMI        |             |
|--|-------------|-------------|
|  | Sensitivity | Specificity |
| 2 $n$                                  | 0.66        | 0.52        |
| 5 $n$                                  | 0.68        | 0.47        |
| 10 $n$                                 | 0.69        | 0.47        |
| 20 $n$                                 | 0.69        | 0.47        |
| 50 $n$                                 | 0.78        | 0.33        |

**Fig. S2. TCGA simulations to test robustness of community parameters.** (a) Performance within and between communities in the TCGA simulations compared to population-level TCGA-LUAD GLasso interactome. Accuracy metrics are averaged across the 50 sampled datasets per cohort size. (b) Performance of REMI when the number of nodes is increased within the community from 2 $n$  to 50 $n$ . Accuracy metrics are averaged across the 50 sampled datasets per cohort size.

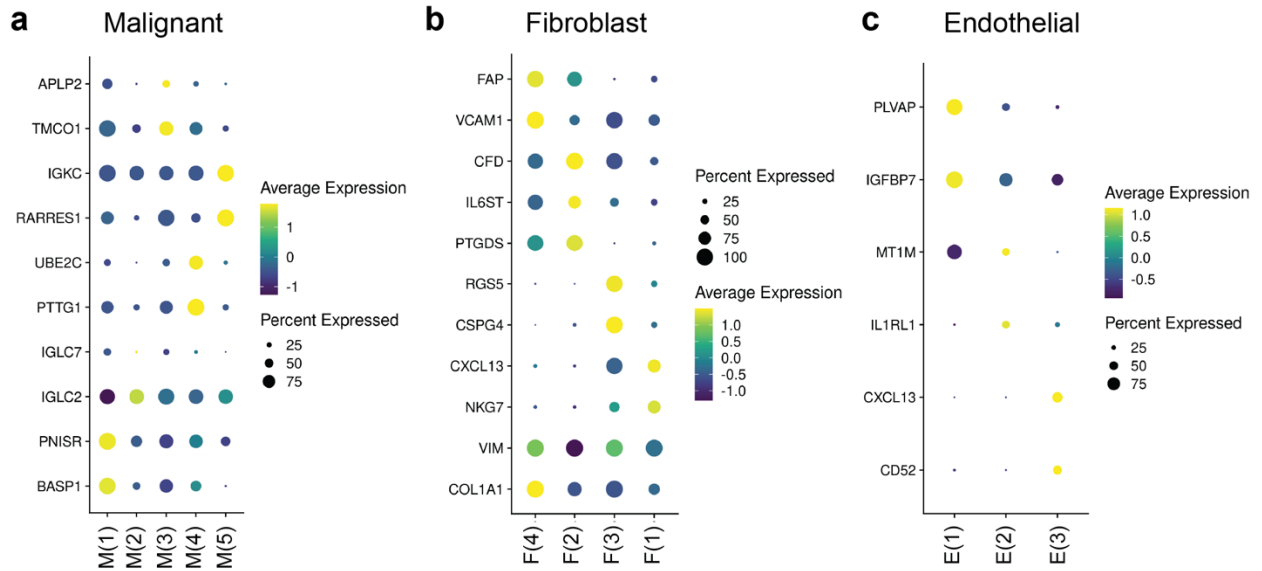


**Fig. S3. Defining TME subpopulation characteristics. (a)** Averaged scaled expression levels of top expressed differentially expressed (DE) markers for each malignant subpopulation **(b)** Averaged scaled expression levels of top expressed DE markers for each fibroblast subpopulation **(c)** Averaged scaled expression levels of top expressed DE markers for each endothelial subpopulation

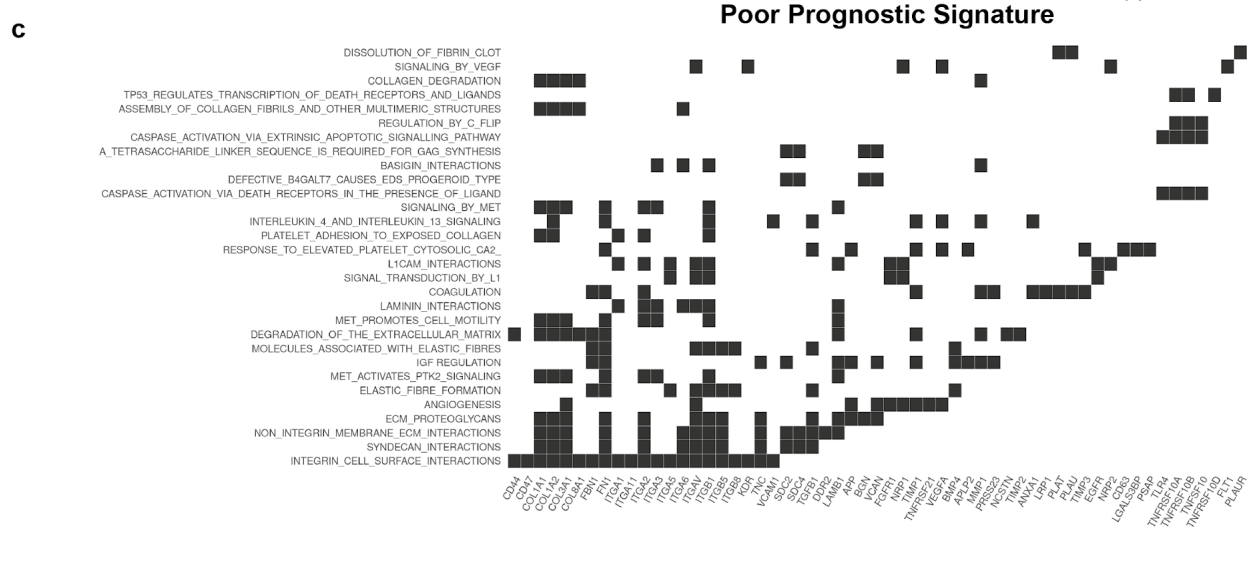
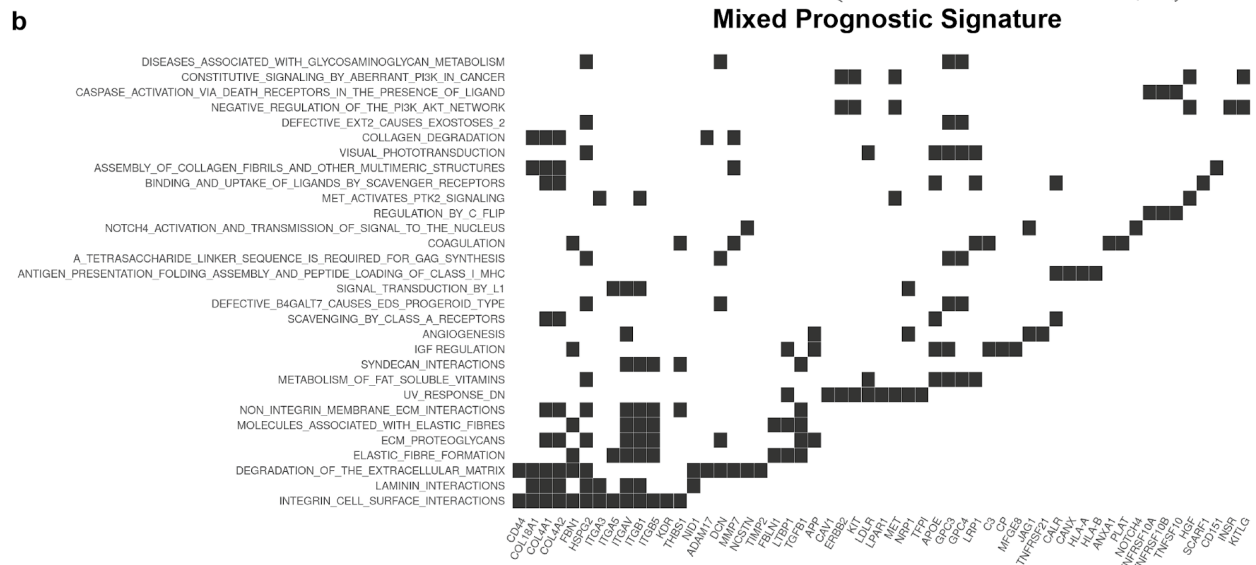
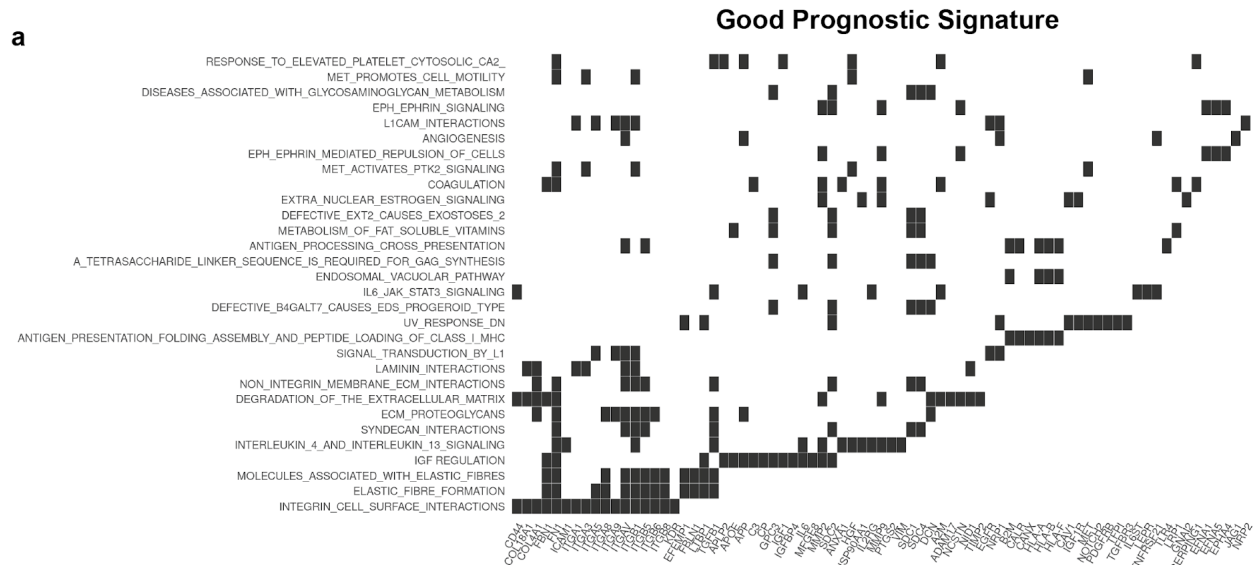
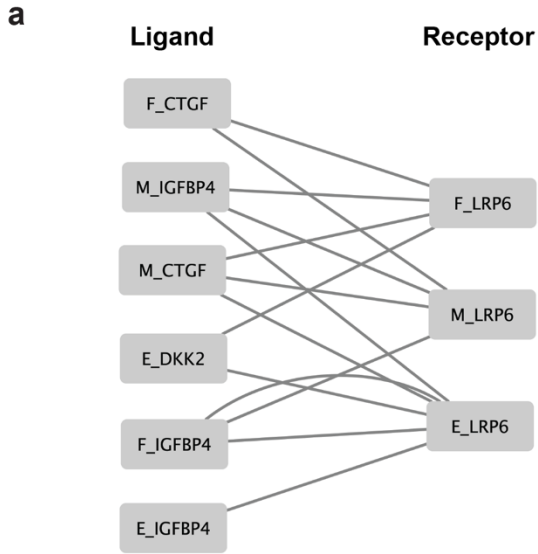


**Fig. S4. Enrichment of prognostic signatures.** (a) Enriched genesets for ligand and receptor genes in good prognostic signature (adj p-value < 0.05, max GS size = 150) (b) Enriched genesets for ligand and receptor genes in mixed prognostic signature (adj p-value < 0.05, max GS size = 150) (c) Enriched genesets for ligand and receptor genes in poor prognostic signature (adj p-value < 0.05, max GS size = 150)



**b**

| Ligand   | Receptor | p-value |
|----------|----------|---------|
| E_DKK2   | E_LRP6   | 0.054   |
| E_IGFBP4 | E_LRP6   | 0.64    |
| F_IGFBP4 | E_LRP6   | 0.12    |
| E_DKK2   | F_LRP6   | 0.01    |
| F_CTGF   | F_LRP6   | NA      |
| F_IGFBP4 | E_LRP6   | 0.12    |
| M_CTGF   | E_LRP6   | 0.94    |
| M_CTGF   | F_LRP6   | NA      |
| M_IGFBP4 | E_LRP6   | 0.15    |
| M_IGFBP4 | F_LRP6   | NA      |
| F_CTGF   | M_LRP6   | 0.059   |
| F_IGFBP4 | M_LRP6   | 0.13    |
| M_CTGF   | M_LRP6   | 0.049   |
| M_IGFBP4 | M_LRP6   | 0.15    |

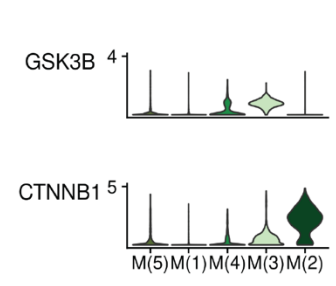
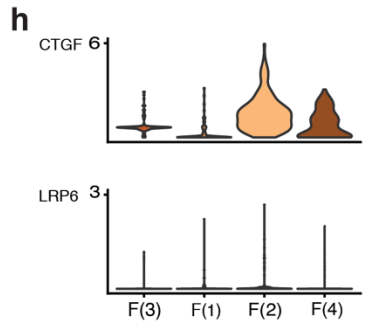
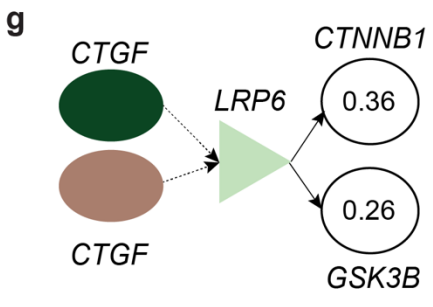
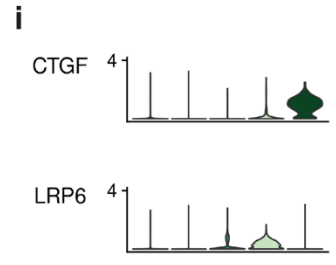
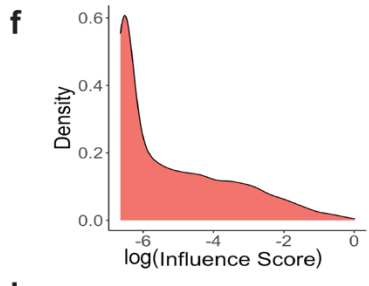
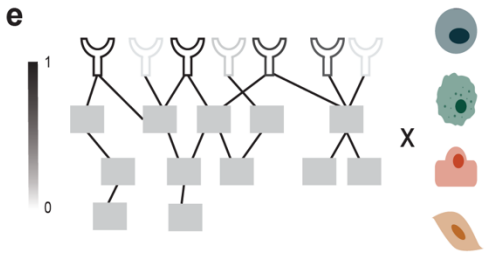
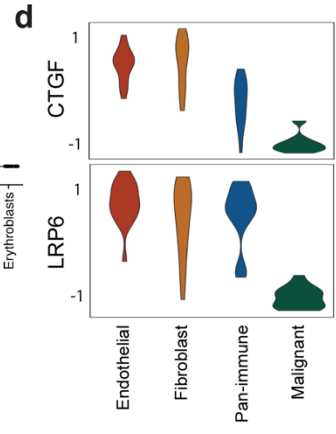
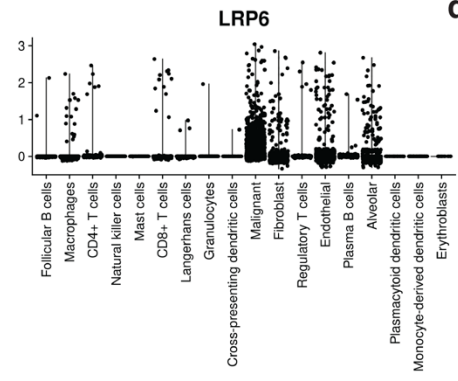
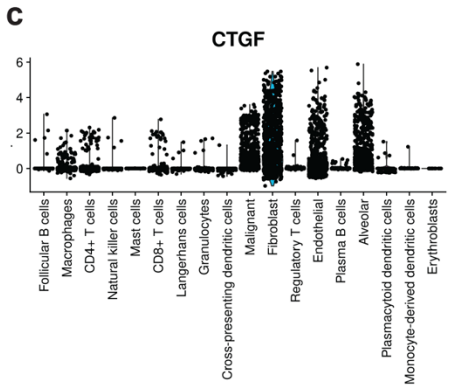


**Fig. S5. CTGF scREMI community characteristics.** (a) Network visualization of the predicted community network (community #50) containing CTGF expressed on malignant cells. Nodes are labeled as celltype\_genename. An edge indicates a predicted LR pair. (b) Table of p-values for each edge. NA represents pairs where perturbing that particular edge did not lead to a converged result. (c) Scaled expression of *CTGF* and *LRP6* across cell types in the single-cell RNA-seq data (d) Scaled expression levels of *CTGF* and *LRP6* across bulk flow-sorted RNA-seq levels (e) Visual diagram of how to calculate downstream receptor score. A downstream signaling pathway network is built for each distinct cell type in the dataset. Eigenvector centrality is calculated for each downstream signaling gene to measure how “activated” they are within the cell-type. (f) Distribution of downstream centrality scores on a log scale for all four downstream signaling pathway networks. (g) *GSK3B* and *CTNNB1* are downstream genes from *LRP6* found in the downstream signaling networks generated by REMI. The number within the node represents the influence score, which represents how correlated the receptor is to its downstream signaling pathway genes. Color of the nodes reflect the subpopulation label. Shape of the node represents the type of gene (solid circle = ligand, solid triangle = receptor, transparent circle = downstream gene). (h) Scaled expression levels of *CTGF* and *LRP6* across fibroblast subpopulations. (i) Scaled expression levels of *CTGF*, *LRP6*, *GSK3B*, and *CTNNB1* across malignant subpopulations.



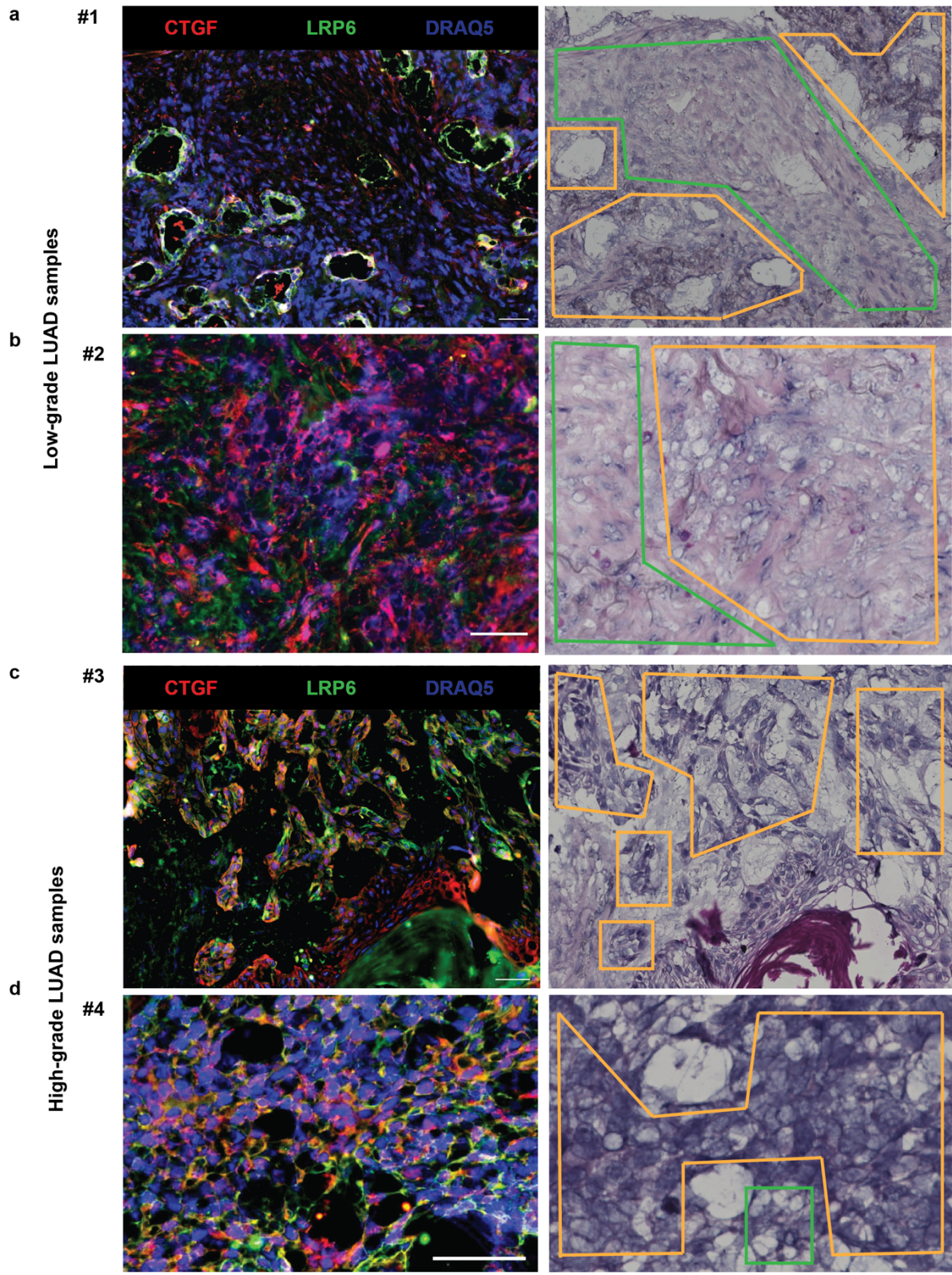


**Fig. S6. Paired immunofluorescence (IF) and H&E images of primary LUAD fresh frozen tissue samples.** H&E images (right) taken after immunofluorescence (IF) staining (left). **On H&E images, regions enriched with malignant versus stromal cells are encapsulated by borders colored orange versus green, respectively.** **(a)** Low-grade sample from LUAD patient #1 showing expression of CTGF and LRP6 expressing cells with low to no co-localization of CTGF and LRP6. **(b)** Low-grade sample from LUAD patient #2 from our lung biobank showing expression of CTGF and LRP6 expressing cells with low to no co-localization of CTGF and LRP6. **(c)** High-grade sample from LUAD patient #3 showing malignant cells with co-expression of CTGF and LRP6 and a small group of malignant cells expressing only CTGF. **(d)** High-grade sample from LUAD patient #4 show co-expression of CTGF and LRP6 in malignant cells. IF images were stained for CTGF (red), LRP6 (green), and DRAQ5 (blue). Scale bar is 50  $\mu$ M. IF images in (a) and (c) are the same as **main-text** Figure 5d, (i) and (ii), respectively.

### Supplementary Data

**Data File 1. REMI\_LUAD\_network.csv.** Table of REMI-LUAD ligand-receptor interactions.

**Data File 2. TCGA-LUAD\_allsamples.csv.** Table of Glasso-derived ligand-receptor interactions from the Cancer Genome Atlas (TCGA) lung adenocarcinoma (LUAD).

**Data File 3. GoodPrognosis\_Interactions.csv.** Table of scREMI-LUAD ligand-receptor interactions associated with good prognosis.

**Data File 4. MixedPrognosis\_Interactions.csv.** Table of scREMI-LUAD ligand-receptor interactions associated with mixed prognosis.

**Data File 5. PoorPrognosis\_Interactions.csv.** Table of scREMI-LUAD ligand-receptor interactions associated with poor prognosis.

**Data File 6. Sample\_Information.docx.** Clinical annotations and histopathological information of LUAD specimens